ADVANCES IN ATMOSPHERIC SCIENCES, VOL. 27, NO. 4, 2010, 937–946

Trends of Temperature Extremes in China and their Relationship with Global Temperature Anomalies

HUANG Danqing (黄丹青), QIAN Yongfu* (钱永甫), and ZHU Jian (朱 坚)

Institute of Severe Weather & Climate, School of Atmospheric Sciences,

Nanjing University, Nanjing 210093

(Received 9 April 2009; revised 9 October 2009)

ABSTRACT

Changes of temperature extremes over China were evaluated using daily maximum and minimum temperature data from 591 stations for the period 1961–2002. A set of indices of warm extremes, cold extremes and daily temperature range (DTR) extremes was studied with a focus on trends. The results showed that the frequency of warm extremes (F_WE) increased obviously in most parts of China, and the intensity of warm extremes (I_WE) increased significantly in northern China. The opposite distribution was found in the frequency and intensity of cold extremes. The frequency of high DTR extremes was relatively uniform with that of intensity: an obvious increasing trend was located over western China and the east coast, while significant decreases occurred in central, southeastern and northeastern China; the opposite distribution was found for low DTR extreme days. Seasonal trends illustrated that both F_WE and I_WE showed significant increasing trends, especially over northeastern China and along the Yangtze Valley basin in spring and winter. A correlation technique was used to link extreme temperature anomalies over China with global temperature anomalies. Three key regions were identified, as follows: northeastern China and its coastal areas, the high-latitude regions above 40°N, and southwestern China and the equatorial eastern Pacific.

Key words: temperature extremes, daily threshold, trend, global temperature anomalies

Citation: Huang, D. Q., Y. F. Qian, and J. Zhu, 2010: Trends of temperature extremes in China and their relationship with global temperature anomalies. *Adv. Atmos. Sci.*, **27**(4), 937–946, doi: 10.1007/s00376-009-9085-4.

1. Introduction

Extreme weather and climate events have various strong impacts on economic and human activities. In the last few years, due to such extreme events, huge losses of human life and exponentially increasing costs associated with weather and climate extremes have often been reported. Therefore, studies on climate change have become increasingly more common, and often focus on climate extremes, including temperature extremes.

Extremes can be defined as values far removed from average conditions, as well as being random in their occurrence. Some traditional methods exist for the detection of temperature extremes. For example, in China, a warm extreme has been defined as a daily maximum temperature over 35°C, and frost days are calculated based on a minimum air temperature of below 0°C (Zhai and Pan, 2003). Experiential statistics based on the climatic characteristics of different regions can also be used to define temperature extremes. For example, due to the special climatic characteristics of southern Canada, temperature thresholds range from 25°C–35°C, except for the milder costal sites where the threshold ranges from 20°C–30°C (Andrew et al., 1999). Today, the most popular methods are percentile and cumulative frequency distribution (CFD) methods (IPCC, 2007). Such as, cold (warm) nights and cold (warm) days have been identified by the 5th and 95th percentiles of the daily minimum and maximum temperature (Bonsal et al., 2001).

As humans and the environment often respond to extremes rather than to mean conditions, it is more important to determine the trends in a range of extreme values, rather than in mean conditions. More-

*Corresponding author: QIAN Yongfu, qianzh2@netra.nju.edu.cn

over, most studies are based on the analysis of trends in climate extremes. On the global scale, a suite of climate change indices exist, which are derived from daily temperature and precipitation data, with a primary focus on extreme events. It has been indicated that over 70% of the global land area has shown a significant decrease in the annual occurrence of cold nights and a significant increase in the annual occurrence of warm nights (Alexander et al., 2006). At the regional scale, significant increases in temperature extremes have been detected through the annual number of hot days and warm nights in Mongolia based on daily maximum and minimum temperature data (Banzragch et al., 2007).

Mean minimum temperature has increased significantly in China during the past 40 years, especially in winter over northern China, while mean maximum temperatures have been found to display no statistically significant trend anywhere in the country (Zhai and Pan, 2003). Decadal means, seasonal cycles, and interannual variations in mean and extreme temperatures have been compared with daily temperatures over eastern China and South Korea during the period 1998–2005 (Li et al., 2009). Previous studies have focused mainly on changes in temperature extremes, with maximum and minimum temperatures considered separately, meaning the total effect by both maximum and minimum temperatures has been ignored. In addition, the methods for defining temperature extremes are too many and need to be more universal.

The present study aims to answer the following questions:

(1) What are the trend distributions of temperature extremes in China, including warm extremes, cold extremes, and daily temperature range (DTR) extremes, as defined by the daily threshold based on both maximum and minimum temperature data?

(2) What are the seasonal trends of different kinds of temperature extremes?

(3) Are there any links between temperature extremes in China and global temperature anomalies? In other words, is regional warming in China spatially or temporally consistent with global temperature anomalies?

The paper is organized as follows. The data used are described in section 2. Section 3 provides a brief description of the different methodologies used, with a particular focus on the definition of warm, cold, and DTR extremes, as well as the different temperature indices. Section 4 describes the trends of the different temperature indices, seasonal trend distributions, and the correlations between temperature extreme indices and global temperature anomalies. Finally, results are summarized and a discussion presented in section 5.

2. Data

Daily data for mainland China from the National Meteorological Information Center, including maximum and minimum daily temperatures, during the period 1961–2002 were used in this study.

Data quality assessment is an important requirement before any calculation or analysis (Craddock, 1979; Hanssen-Bauer and Førland, 1994; Tuomenvirta, 2001; Begert et al., 2005). Aside from some common errors, such as problems associated with temporal inhomogeneity, stations with serious relocation problems were removed. In addition, each station with missing values amounting to more than 5% of the total daily data was removed as well.

Following the above mentioned quality control, a high-quality dataset from 591 stations was established for the study. The data had good spatial coverage over mainland China, and all the stations selected for the study are plotted in Fig. 1.

The global temperature data used for the analysis were from the NCEP/NCAR (National Centers for Environmental Prediction/National Center for Atmospheric Research) reanalysis monthly mean datasets for the period 1961–2002, gridded at 2.5°×2.5° resolution.

3. Methods

3.1 *Definition of temperature extremes*

Based on daily maximum and minimum temperature data from the selected stations in China using the CFD method, the daily higher and lower thresholds for daily extremes of maximum temperature, minimum temperature, and DTR were defined by the 90th and 10th percentiles ($T_{\max 90}$, $T_{\min 90}$, DTR_{90}; $T_{\max 10}$,

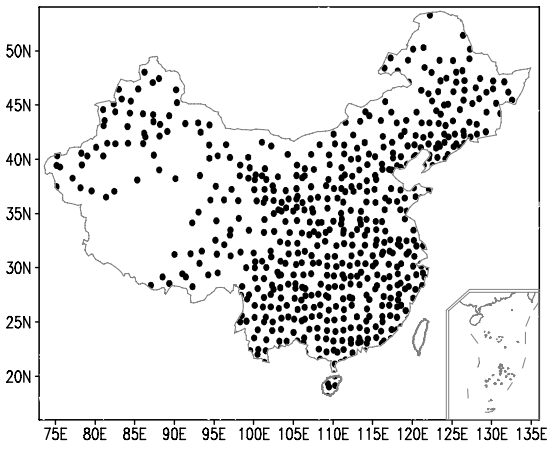

Fig. 1. Locations of the selected stations across China used to supply daily temperature data.

$T_{\min 10}$, DTR_{10}).

In order to analyze temperature extremes comprehensively and in more detail, a threshold was defined respectively for each day during a year. It was found that the threshold on the daily scale (day threshold, for short) contained systematic temperature anomalies. To remove them, and allow the temperature threshold to follow the variance of solar altitude angle, smoothing was necessary. Since the timescale of a weather system is usually around seven days, low-pass filtration was used to omit waves which took less than eight days to be induced by weather disturbances. Finally, obtaining a more reasonable day threshold depended on seasonal advances to define temperature extremes (Huang and Qian, 2008).

Usually, on warmer days, both the daily maximum temperature and minimum temperature are higher, and vice versa. Based on the percentage (figure omitted) between days upon which both the daily maximum and daily minimum temperatures were higher (lower), and the total days during the period 1961–2002, the values of all stations were above 80%. This means that in most cases a higher maximum temperature during the day was usually followed by a warm night, and vice versa. Thus, in this paper, the authors have focused on warm extremes defined as both the daily maximum and daily minimum temperatures which were equal to or greater than $T_{\max 90}$ and $T_{\min 90}$ on the same day, and cold extremes defined as both being equal to or less than $T_{\max 10}$ and $T_{\min 10}$.

The DTR, which means the difference between daily maximum and minimum temperatures, is to some extent the clearest indicator of the kind of temperature variability experienced under global warming. This is because the DTR contains information on both maximum and minimum temperatures. DTR extremes have been identified in this paper, which contain high DTR extremes defined as DTR above DTR_{90} and low DTR extremes defined as DTR below DTR_{10}.

Table 1. Definition of temperature extremes indices. $T_{\max}$ and $T_{\min}$ are daily maximum and minimum temperature, respectively.

Indicator name	Definitions	Units
Warm extremes frequency (F_WE)	No. of days (per year) with $T_{\max} \geqslant T_{\max 90}$ and $T_{\min} \geqslant T_{\min 90}$	d
Warm extremes intensity (I_WE)	Temperature above thresholds of $T_{\max 90}$ and $T_{\min 90}$: $\sum_{\text{per\_year}} (T_{\max} - T_{\max 90} + T_{\min} - T_{\min 90})/F\_\mathrm{WE}$	°C d^{-1}
Cold extremes frequency (F_CE)	No. of days (per year) with $T_{\max} \leqslant T_{\max 10}$ and $T_{\min} \leqslant T_{\min 10}$	d
Cold extremes intensity (I_CE)	Temperature below thresholds of $T_{\max 10}$ and $T_{\min 10}$: $\mathrm{abs}\left(\sum_{\text{per\_year}} (T_{\max} - T_{\max 10} + T_{\min} - T_{\min 10})/\mathrm{F\_CE}\right)$*	°C d^{-1}
High DTR extremes frequency (F_HD)	No. of days (per year) with DTR$\geqslant$DTR$_{90}$	d
High DTR extremes intensity (I_HD)	DTR above threshold DTR_{90}: $\sum_{\text{per\_year}} (\mathrm{DTR}-\mathrm{DTR}_{90})/\mathrm{F\_HD}$	°C d^{-1}
Low DTR extremes frequency (F_LD)	No. of days (per year) with DTR$\leqslant$DTR$_{10}$	d
Low DTR extremes intensity (I_LD)	DTR below threshold DTR_{10}: $\mathrm{abs}\left(\sum_{\text{per\_year}} (\mathrm{DTR}-\mathrm{DTR}_{10})/\mathrm{F\_LD}\right)$	°C d^{-1}

*As $(T_{\max} - T_{\max 10} + T_{\min} - T_{\min 10})$ is a negative value, abs $(T_{\max} - T_{\max 10} + T_{\min} - T_{\min 10})$ was used to identify the intensity of temperature extremes, as in the I_LD index.

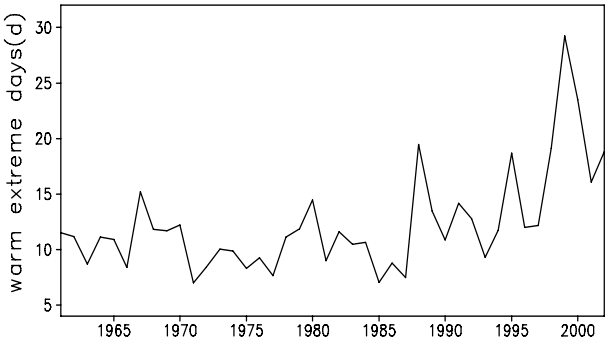

Fig. 2. Averaged numbers of warm extreme days for the period 1961–2002 in China.

3.2 *Indices of temperature extremes*

A set of eight temperature extreme indices was selected for this study and their descriptions are given in Table 1. All the indices were analyzed and presented by daily maximum and minimum temperatures.

3.3 *Statistical methods*

Linear trends were estimated using linear regression modeling. The EOF technique was used to identify the spatial and temporal patterns of temperature extreme anomalies. The associations between temperature extreme anomalies and global temperature anomalies were established by correlation.

4. Results

4.1 *Trends in temperature extremes*

4.1.1 *Warm extremes*

Figure 2 shows the variation in the average number of extreme warm days in China. For China as a whole, there was a slight decreasing trend prior to the mid-1980s, but a sharp increasing trend was apparent thereafter. From the 1960s to the mid-1980s, the number of extreme warm days was 8–15 days per year, while up to the year 2000, this figure reached 28 days per year.

Figure 3 presents a map of the statistically significant trends in the warm extreme indices (shown in Table 1). The spatial trend distribution of F_WE (Fig. 3a) indicates there were significant increases in most parts of China, especially in the north and southeast of the country. As shown in Fig. 3b, a remarkable decreasing trend of I_WE was found mainly in southeastern China. However, stations with obvious increasing trends were mostly located in central and western China, especially in Inner Mongolia (35°–45°N, 95°–115°E). In conclusion, stations with significant trends in F_WE were mostly located in eastern China, and stations in interior China had smaller and non-significant trends.

Comparing the trends of F_WE and I_WE, F_WE increased obviously in northern China and South China, while the opposite trend distribution was found in I_WE in South China. In addition, in the northwestern part of Xinjiang Province (35°–50°N, 75°–95°E) and in Inner Mongolia, both F_WE and I_WE showed remarkable increasing trends. This means there was no synchronous variance between the frequency and intensity of warm extremes in the whole of China.

This relationship depended on regional characteristics. According to the definition of the intensity of warm extremes, if the total cumulative temperature amounted to more than the threshold, then the intensity would be smaller when the frequency increases during a given period in a given region or regions. The phenomenon of the non-accordance of variance between F_WE and I_WE means that, although the

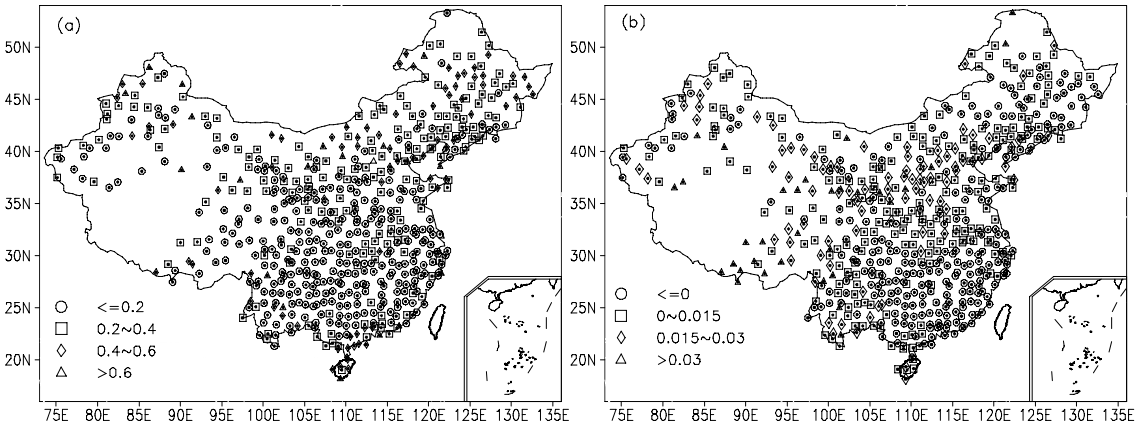

Fig. 3. Spatial distribution of trends (circles with a dot inside indicate a statistical significance at the 0.05 level) for (a) F_WE (units: d) and (b) I_WE (units: $^{\circ}$C d^{-1}) of warm extreme days in China during 1961–2002.

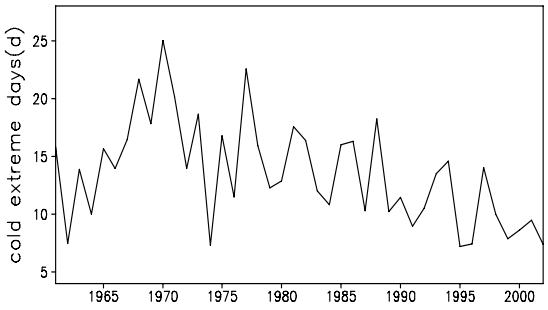

Fig. 4. Averaged numbers of cold extreme days during 1961–2002 in China.

number of warm extremes increases, the intensity of temperature decreases, indicating that the temperature is not so high as before.

4.1.2 *Cold extremes*

Figure 4 shows the decline in the number of cold extreme days for the whole China in the period 1961–2002. The decreasing trend was especially obvious after the 1980s, while a significant increasing trend was found from the mid-1960s to the mid-1970s.

As Fig. 5a shows, a remarkable decreasing trend of F_CE was concentrated in some parts of southwestern China, while in the northwestern part of western China and throughout most of southern China, especially along the coastline, F_CE decreased slightly. I_CE (shown in Fig. 5b) decreased significantly, mainly in Inner Mongolia and the lower reaches of the Yellow River basin. However, stations with a remarkable increasing trend were located in southwestern China and along the southeastern coast. With regard to southern China, while the F_CE was decreasing, the I_CE increased significantly. This means that the average intensity of cold extremes over southern China has increased at a notable rate.

4.1.3 *DTR extremes*

For China as a whole, the total annual number of high DTR extreme days (Fig. 6) displayed a significant declining trend during 1961–2002, especially after the 1980s, whereas the annual number of low DTR extreme days increased obviously. The number of high DTR extreme days was changing from 36 to 58 days per year, while up to 1986 it reached the lowest, 28 days per year. The number of low DTR extreme days increased from 1961–2002, and in 1990 the number even reached 51 days per year.

Figure 7 presents a map of the slopes of the regressive equation for the DTR extreme indices (shown in Table 1). With respect to the trend distributions of warm and cold extremes, the significant regions were wider. Decreasing trends were found in most parts of China. The spatial distribution of the slopes of the regression equation for F_HD (Fig. 7a) suggests that F_HD increased significantly along the eastern coast and in some parts of western China. Meanwhile, an obvious decreasing trend appeared mainly in central, southeastern and northeastern China, especially in the northern parts of northeastern China. Figure 7b shows that declining trends in F_LD were mainly located in the northern part of Inner Mongolia, while a remarkable increasing trend was found in western parts of western China, northern China and some areas of southern China. The trend pattern of I_HD (figure omitted) and I_LD (figure omitted) were consistent with the trends in F_HD and F_LD, respectively.

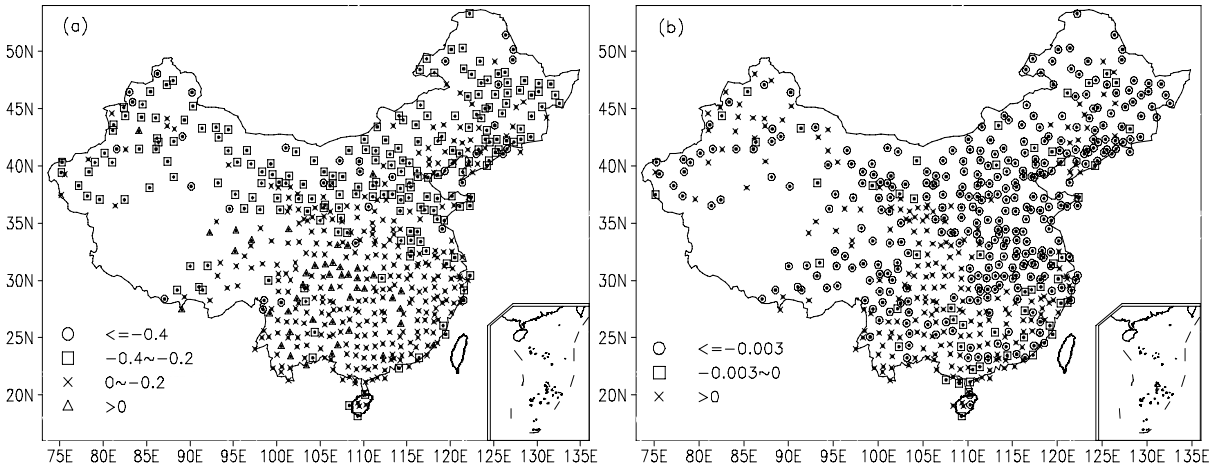

Fig. 5. Spatial distribution of trends (circles with a dot inside indicate statistical significance at the 0.05 level) for (a) F_CE (units: d) and (b) I_CE (units: °C d^{-1}) of cold extreme days in China during 1961–2002.

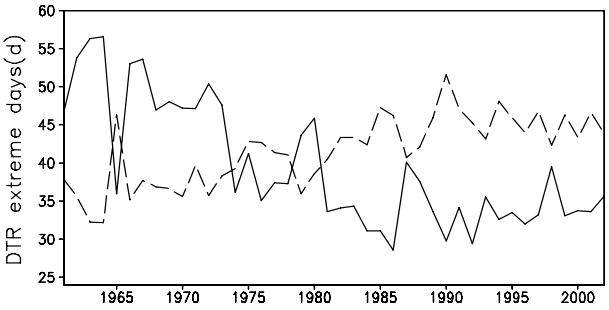

Fig. 6. Averaged numbers of high DTR extreme days (solid lines) and low DTR extreme days (dashed lines) during 1961–2002 in China.

4.2 *Seasonal trend in temperature extremes*

Trends in temperature extremes over China also exhibited remarkable seasonal differences. In spring (Fig. 8a), the significant increasing trend was concentrated in northern China and the lower reaches of the Yangtze River Basin. Stations with an obvious trend were few in summer (Fig. 8b). The significant trend in autumn was in accordance with that in winter: the distribution demonstrates that stations with a significant increasing trend were located mostly in northern China. The spatial distribution of I_WE (figure omitted) was consistent with F_WE. According to the cold extremes, the significant increasing trend of F_CE occurred over southern China in spring, while in other seasons the trend was not obvious. I_CE indicated remarkable increasing trends over southern China and northwestern Xinjiang in spring. A significant increasing trend was found along the Yangtze River valley in summer, and the obvious decreasing trend was located over northeastern China in autumn, while in winter the trend was not significant.

Comparing seasonal trends in DTR extremes (figure omitted), F_HD and I_HD showed similar patterns. A significant increasing trend over most parts of southern China was indicated, especially in spring and autumn, while an obvious decreasing trend was found in northeastern China in spring and in southwestern parts of China in winter. However, the seasonal trends of F_LD and I_LD presented opposite distributions to those of F_HD and I_HD, respectively.

4.3 *Associations between temperature extreme anomalies in China with global temperature anomalies*

In order to find out whether regional warming over China is spatially or temporally consistent with global temperature variations, and, if a relationship exists, where the key region is and when the key time is, the correlation technique was performed jointly on temperature extreme anomalies over China and global temperature anomalies during the period 1961–2002. As the spatial distributions of F_CE (figure omitted) and F_WE exhibited very similar but opposite-signed patterns, F_WE was taken as an example for estimating the associations.

First, the anomalies of warm extremes over China were picked out by the EOF technique. EOF analysis was performed on the F_WE anomalies over China for the period 1961–2002. The variances of the first three modes were 47%, 10% and 5%, respectively, contributing more than 62% of the total variance. This suggests that the three modes can describe most variations in warm extremes. Their corresponding time coefficients, measured in units of their respective standard deviations (denoted as PC1, PC2, and PC3, respectively), are plotted in Fig. 9.

The first spatial pattern of the F_WE (Fig. 9a)

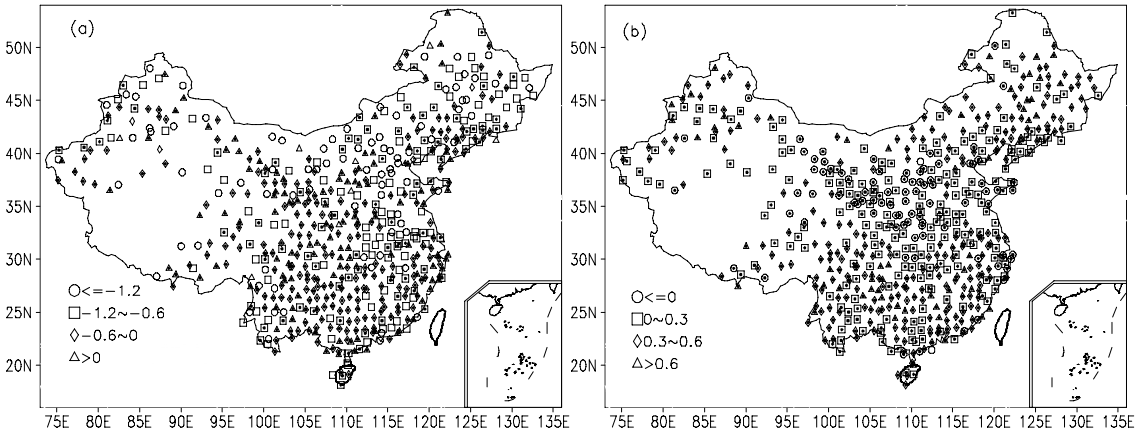

Fig. 7. Spatial distribution of trends (circles with a dot inside indicate statistical significance at the 0.05 level) for (a) F_HD (units: d), (b) F_LD (units: °C d^{-1}) of DTR extremes in China during 1961–2002.

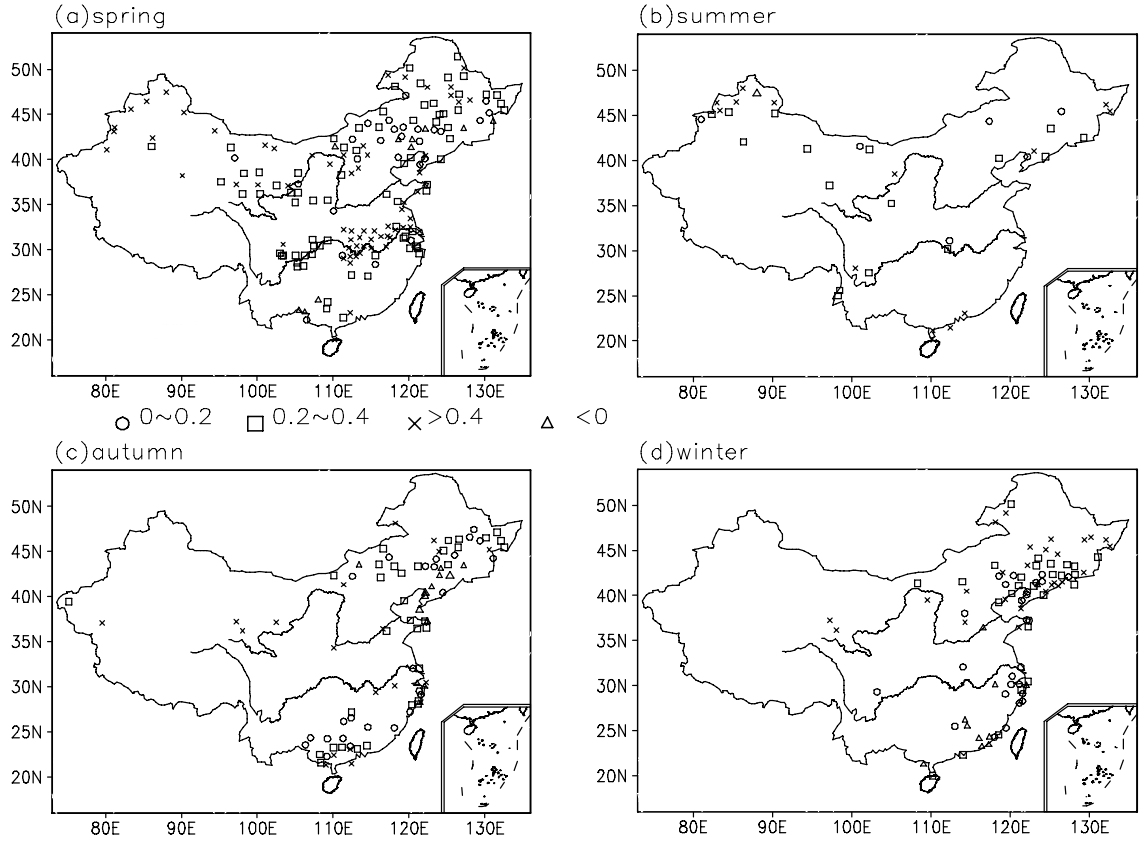

Fig. 8. Spatial distribution of seasonal trends of F_EW (units: d) in China during 1961–2002: (a) spring; (b) summer; (c) autumn; (d) winter (stations with significant trends indicated in the figures).

a consistent variation pattern for the whole of China. The F_WE anomalies over China indicated the same variation, with the largest value in Inner Mongolia. The second spatial pattern (Fig. 9c) indicates a "+−" pattern spanning from northern China to southern China. This means that the second mode showed a converse variance pattern between southern China and northern China. The third spatial pattern (Fig. 9e) indicates a weakened/strengthened pattern in the middle part of China. Figures 9b, 9d, and 9f give the time series of PC1, PC2 and PC3, respectively. PC1 indicates a significant increasing trend, especially after the 1990s. PC2 suggests a significant decadal pattern, with the point of change having been around the mid-1970s. PC3 depicts an obvious increasing trend before the 1990s and a decreasing trend thereafter. The change point was around 1990.

Figures 10a–10c show the correlation distributions of same-period global temperature anomalies against the normalized PC1, PC2, and PC3, respectively. Values with a magnitude greater than the 95% confidence level are shaded. The correlation distribution between global temperature anomalies and the normalized PC1 is shown in Fig. 10a. While temperature extreme anomalies over China showed the same variation pattern, temperature anomalies in most parts of the world showed a positive correlation, with significant large values in two areas: eastern China and its coastal areas, and northern Canada, especially in northeastern China and its coastal areas. Figure 10b shows the correlation pattern against PC2 and depicts a significant positive correlation concentrated in the high-latitude regions above 40°N and an obvious negative correlation concentrated in southwestern China. The correlation pattern against PC3 (Fig. 10c) depicts that while the F_WE strengthens/weakens in mid China, significant positive values concentrated in the equatorial eastern Pacific, especially in the Niño3.4 region. This correlation distribution demonstrates the anomalous patterns with F_WE strengthened/weakened in mid China were related to the Pacific decadal oscillation (PDO) pattern. The correlation coefficients between PC3 serial and the PDO index was as high as 0.82.

5. Discussion and conclusions

Based on daily maximum and minimum tempera-

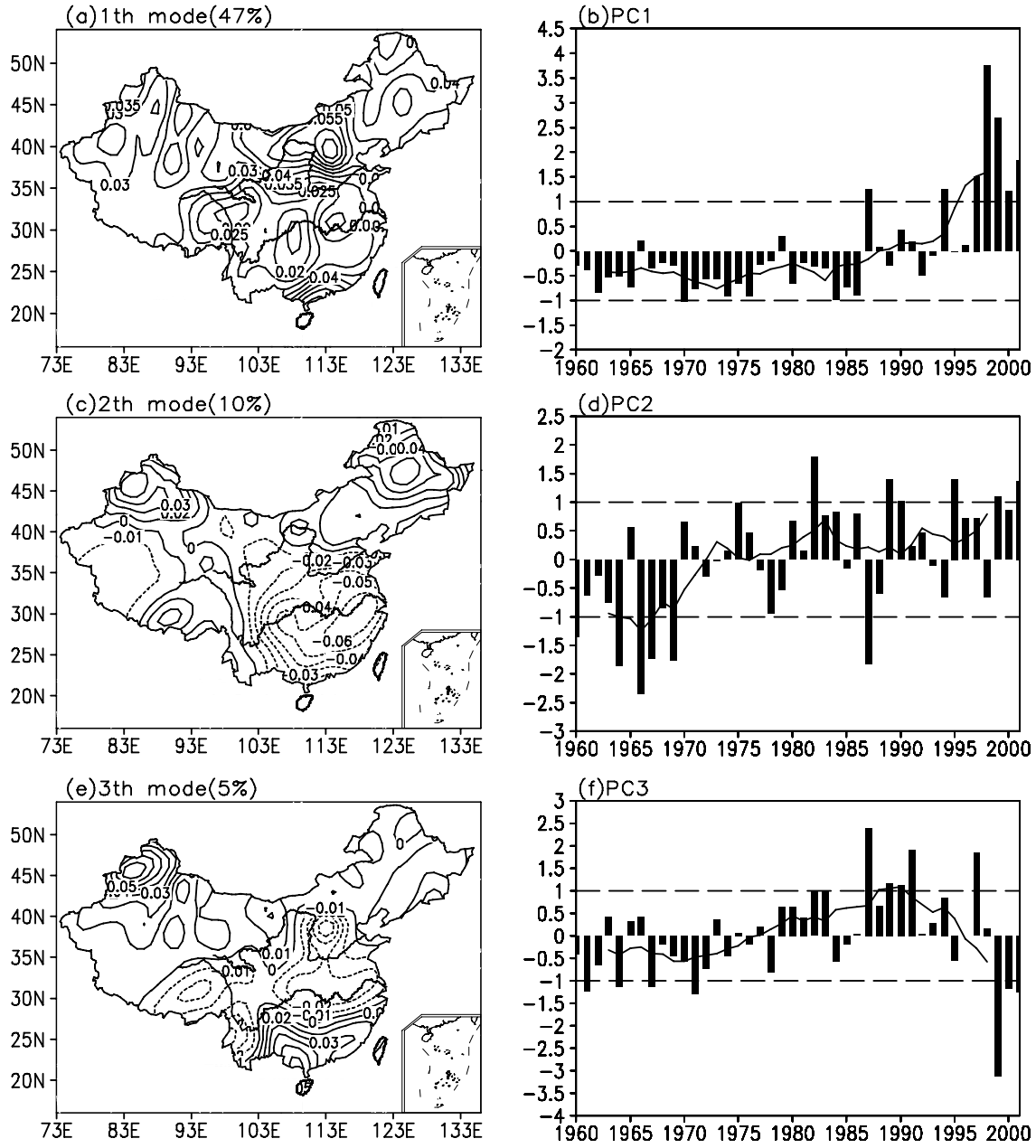

Fig. 9. Spatial patterns (a, c, and e) and time coefficients (b, d, and f) of the first three EOF leading modes of the F_WE. The time coefficients (bars) are measured in units of their respective standard deviations. Lines are the 10-running average results.

ture data in China from 1961–2002, trends in the frequency and intensity of warm extremes, cold extremes and DTR extremes have been analyzed in this paper.

The results showed that F_WE increased remarkably in most parts of China, and a significant increasing trend in I_WE was found in northern China. However, trends in F_CE and I_CE were opposite. The trend distribution for F_HD was consistent with I_HD: an obvious increasing trend concentrated along the eastern coast and in western China, while a decreasing trend was located mainly in central, southeastern and northeastern China. Opposite distributions were found for F_LD and I_LD. Since the significant trends for those stations close to the eastern coastline were different with those for northern China, future work could involve an analysis of the correlation between sea surface temperature and temperature extremes in China.

Seasonal trends indicated that F_WE and I_WE increased significantly, especially over northeastern

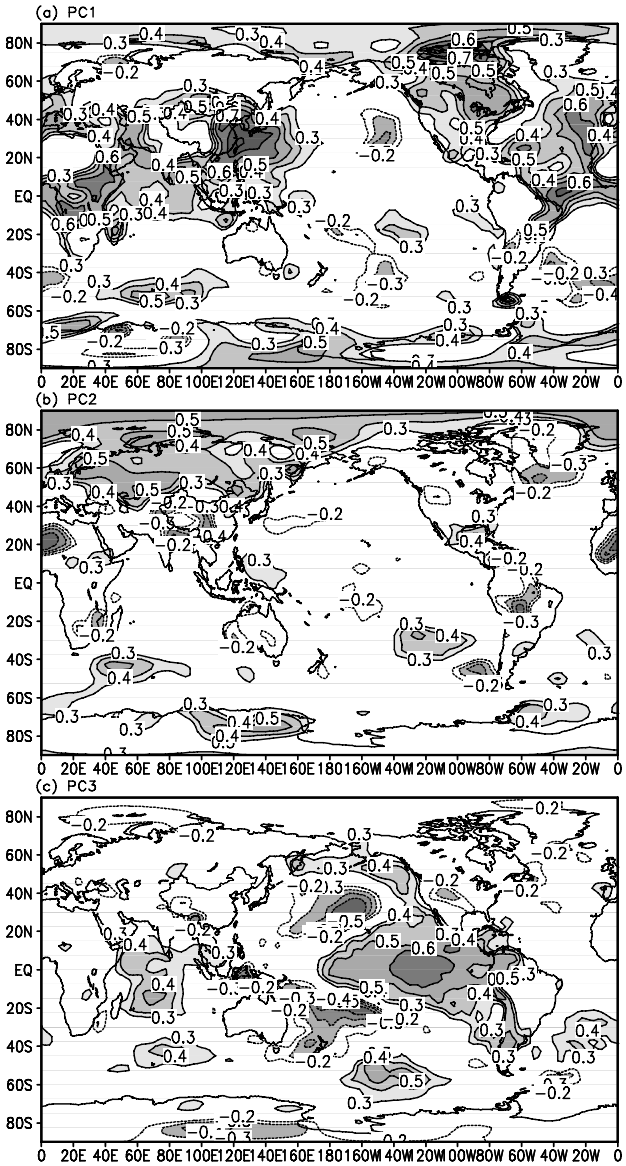

Fig. 10. Correlation distributions of PC1, PC2 and PC3 with global temperature anomalies. Values with a magnitude greater than the 95% confidence level are shaded.

China and along the Yangtze River valley in spring and winter. The distribution of F_CE was consistent with I_CE: An increasing trend was located in northwestern China and southern China in spring, while an obvious decreasing trend was found in northeastern China in autumn. Seasonal trends in DTR extremes, including both F_HD and I_HD, increased in southern China and decreased in northeastern China, especially in spring and autumn; the opposite distribution was found for F_LD and I_LD.

A correlation technique was performed to link temperature extremes (i.e. F_WE) with global temperature anomalies. It can be concluded that, while temperature extreme anomalies over China showed a pattern of consistent variation, most parts of the world showed a positive correlation distribution, especially in northeastern China and its coastal areas.

Furthermore, PC2 demonstrated clear interdecadal variations (Wang, 2001; Yu et al., 2004; Li et al., 2005; Xin et al., 2006; Yu and Zhou, 2007, Zhou et al., 2009), with the climate transition being around the late 1970s. The correlation distribution against PC2 demonstrated a significant positive correlation concentrated in the high-latitude regions above 40°N, with southwestern China showing an obvious negative correlation.

Finally, the correlation pattern against PC3 indicated that, while the F_WE strengthened/weakened in mid China, significant positive values concentrated in the equatorial eastern Pacific, especially in the Niño3.4 region (5°N–5°S, 170°–120°W). The PC3 serial was related to the PDO pattern, as the correlation between PC3 and the PDO index was as high as 0.82.

Many studies have shown differences in the circulation response to changes in the circumglobal teleconnection pattern in the mid-latitude circulation of the Northern Hemisphere, related to a different response of ENSO (Ding and Wang, 2005). The temperature extremes in southern Argentina are also closely related to the warming and cooling of the coastal waters in the South Atlantic and South Pacific (Rusticucci et al., 2003). These results suggest there is a need for better understanding of the relationship between large-scale oscillations, including ENSO, the North Atlantic Oscillation (NAO), PDO, and the variability of extreme events in China.

Acknowledgements. This work was supported by the National Natural Science Foundation of China under Grant Nos. 40675042, 40901016 and 40805041. The authors appreciate the insightful comments and suggestions from the three anonymous reviewers.

REFERENCES

Alexander, L., and Coauthors, 2006: Global observed changes in daily climate extremes of temperature and precipitation. *J. Geophys. Res.*, **111**(D05109), doi: 10.1029/2005JD006290.

Andrew, F., E. David, and W. Bryan, 1999: Climate variability and the frequency of extreme temperature events for nine sites across Canada: Implications for power usage. *J. Climate*, **12**, 2490–2502.

Banzragch, N., G. Scott, and G. Clyde, 2007: Trends in extreme daily precipitation and temperature near lake Hövsgöl Mongolia. *International Journal of Climatology*, **27**, 341–347.

Begert, M., T. Schlegel, and W. Kirchhofer, 2005: Homogeneous temperature and precipitation series of Switzerland from 1863 to 2000. *International Journal of Climatology*, **25**, 65–80.

Bonsal, B., X. Zhang, L. Vincent, and W. Hogg, 2001: Characteristics of daily and extreme temperatures over Canada. *J. Climate*, **14**, 1959–1976.

Craddock, J., 1979. Methods for comparing annual rainfall records for climate purposes. *Weather*, **34**, 332–346.

Ding, Q., and B. Wang, 2005: Circumglobal teleconnection in the Northern Hemisphere Summer. *J. Climate*, **18**, 3483–3505.

Hanssen-Bauer, I., and E. Førland, 1994: Homogenizing long Norwegian precipitation series. *J. Climate*, **7**, 1001–1013.

Huang, D., and Y. Qian, 2008: The definition of daily mean temperature extremes over China and its trend. *Acta Scientiarum Naturalium Universitatis Sunyatseni*, **47**(3), 112–116. (in Chinese)

IPCC, 2007: *Climate Change 2007: Observations: Surface and Atmospheric Climate Change*. Solomon et al., Eds., Cambridge University Press, 336pp.

Li, H., T. Zhou, and J. Nam, 2009: Comparison of daily extreme temperatures over eastern China and South Korea between 1996–2005. *Adv. Atmos. Sci.*, **26**, 253–264, doi: 10.1007/s00376-009-0253-3.

Li, J., R. Yu, T. Zhou, and B. Wang, 2005, Why is there an early spring cooling shift downstream of the Tibetan Plateau. *J. Climate*, **18**, 4660–4668.

Rusticucci, M., S. Venegas, and W. Vargas, 2003: Warm and cold events in Argentina and their relationship with South Atlantic and South Pacific Sea surface temperatures. *J. Geophys. Res.*, **108**(D3356), doi: 10.1029/2003JC001793.

Tuomenvirta, H., 2001: Homogeneity adjustments of temperature and precipitation series-Finnish and Nordic data. *International Journal of Climatology*, **21**, 495–506.

Wang, H., 2001: The weakening of Asian monsoon circulation after the end of 1970's. *Adv. Atmos. Sci.*, **18**, 376–386.

Xin, X., R. Yu, T. Zhou, and B. Wang, 2006; Drought in late spring of South China in recent decades. *J. Climate*, **19**, 3197–3206.

Yu, R., B. Wang, and T. Zhou, 2004: Tropospheric cooling and summer monsoon weakening trend over East Asia. *Geophys. Res. Lett.*, **31**(L22212), doi: 10.1029/2004GL021270.

Yu, R., and T. Zhou, 2007: Seasonality and three-dimensional structure of the interdecadal change in East Asian monsoon. *J. Climate*, **20**, 5344–5355.

Zhai, P., and X. Pan, 2003: Trends in temperature extremes during 1951–1999 in China. *Geophys. Res. Lett.*, **30**, doi: 10.1029/2003GL018004.

Zhou, T., R. Yu, J. Zhang, J. Li, and X. Xin, 2009: Why the western Pacific subtropical high has extended westward since the late 1970s. *J. Climate*, **22**, 2199–2215.